Pak. J. Bot., 55(5): 1827-1839, 2023. DOI: http://dx.doi.org/10.30848/PJB2023-5(19)

METABOLOMIC ANALYSIS OF SEED COAT AND PEELED SEEDS OF *POLYGONATUM CYRTONEMA* IN SAND STORAGE

WENWU ZHANG[#], JINFENG TONG[#], CHENYU SONG, FULEI PENG, XU YANG AND QING JIN[*]

School of Life Sciences, Anhui Agricultural University, Hefei 230036, China
[*]Corresponding author's email: qingjin@ahau.edu.cn

Abstract

The ending of seed dormancy by sand storage involves complex interactions in cells. To assess the effect of sand storage on dormancy breaking in seeds of *Polygonatum cyrtonema* Hua, the seed germination rate and metabolites change were monitored in seed coat and peeled seeds. The germination rate of *P. cyrtonema* seeds was increased after 60 d of storage at 4°C or room temperature -5 to 15°C. Metabolomics analysis showed that there were 85 and 74 metabolites in seed coat and peeled seeds, respectively. The dynamic changes in metabolites and in metabolic pathways during sand storage were analyzed by the principal component analysis (PCA) and orthogonal partial least squares-discriminant analysis (OPLS-DA) models. Metabolomics analysis showed that sand storage had different effects on the seed coat and peeled seeds. The tricarboxylic acid (TCA) cycle, amino acid metabolism, and gluconeogenesis of the peeled seeds were active in sand storage for 30 d and 60 d, which provided energy for seed germination. Myo-inositol and γ-aminobutyric acid (GABA), molecules related to seed germination, were also affected in the sand storage process. These results provide a comprehensive analysis of the metabolic changes for exploring the seed dormancy mechanism of *P. cyrtonema*.

Key words: *Polygonatum cyrtonema* Hua, Sand storage, Seed germination, Metabolic profiling, GC-MS.

Introduction

Plants of *Polygonatum* genus, especially *Polygonatum cyrtonema* Hua (*P. cyrtonema)*, are traditional Chinese medicinal herbs that are used to treat disorders of the lung, kidney, and spleen and, more importantly, to prevent aging (Ma *et al*., 2021). The major active ingredients of *P. cyrtonema* are polysaccharide (Xie *et al*., 2021) which improve their market demand. At present, the reproduction of *P. cyrtonema* mainly depends on the rhizome, which is wasteful. Long-term asexual reproduction causes germplasm degradation and thereby leads to diseases and insect pests related problems. Due to higher seed production of *P. cyrtonema*, its seeds reproduction can be used for the management of above problems effectively with reduced production costs level. However, the *P. cyrtonema* seed germination rate is low in natural environments, resulting in a huge waste of seed resources. The seeds of *P. cyrtonema* show comprehensive dormancy (Zhang *et al*., 2010) which prevents seeds from germinating under unfavorable physical conditions. In many wild species, seeds are dormant at maturity and do not germinate until dormancy release after dispersal, even after exposed to optimal conditions (Chen *et al*., 2020; Zhang *et al*., 2022). Germination is a complex trait that is influenced by endogenous and environmental factors (Zhang *et al*., 2020; Chen *et al*., 2022). There are many methods including chemical, biological, and physical methods to alleviate seed dormancy (Kosa & Karaguzel, 2020; Abo-Hamad, 2021). Among them, low-temperature sand storage are the most common methods to end the seed dormancy (Wang *et al*., 2019).

To further investigate the metabolic changes during low-temperature sand storage, metabolomic approaches have been employed. For example, GC-MS has been used to reveal the dynamic changes in metabolites of the wheat embryo and endosperm during seed germination (Han *et al*., 2017). GC-MS has been applied to identify and ensure the quality of the Chinese medicinal materials *Dendrobium officinale* and *Dendrobium huoshanense* during different growth years (Jin *et al*., 2016). Recently, metabolomic characterization based on the nontargeted GC-MS of seed germination has been reported (Rubab *et al*., 2020; Qi *et al*., 2022).

In the present study, the seeds of *P. cyrtonema* were used as raw materials. The effects of sand storage time and temperature on the seed germination of *P. cyrtonema* were studied. Further, the metabolites in the seed coat and peeled seeds of *P. cyrtonema* at different sand storage times were studied by GC-MS.

Materials and Methods

Plant material and burial: The *P. cyrtonema* seeds were collected from the Huangjing planting base in Qingyang County, Anhui, China in September 2016. Pure sand and seeds were mixed at a ratio of 3:1 in a foam box to make a layer of fine sand and a layer of seed. The seed samples were stored at -20°C, 4°C, and 26°C or room temperature -5 to 15°C. The samples were sprayed with water regularly to maintain their moisture level at 60–80%. The seeds were collected at four different sand storage stages, i.e., at 0 d (non-sand storage, ck), 30 d, 60 d, and 90 d. The seed coats and peeled seeds were separated and stored at -80°C prior to metabolite extraction.

Determination of seed activity and embryo rate: The seeds of *P. cyrtonema* were soaked in warm water for 24 h, then cut along the longitudinal axis of the embryo. The seeds were stained with 0.2% full name (TTC) solution in a 25°C incubator for 24 h. Then the seeds were cleaned and observed for the dyeing of embryo and endosperm. At the same time, half of the seeds with more embryos were selected, and their longitudinal axis length (i.e., endosperm length) was measured with Vernier calipers. Embryo sections were observed under microscope for embryo length and the embryo rate was calculated.

$$\text{Seed activity} = \frac{\text{Dyed seeds}}{\text{Total number of seeds}} \times 100\%$$

$$\text{Embryo rate} = \frac{\text{Embryo length}}{\text{endosperm length}} \times 100\%$$

Seed germination test: The seeds of *P. cyrtonema* with different sand storage pretreatments were taken out, planted in the hole seedling tray and cultured in a constant-temperature incubator at 26°C. For this, one hundred seeds per treatment were used in triplicates. SPSS19 software was used for data statistical analysis. The germination percentage was calculated using the following formula:

$$\text{Germination percentage} = \frac{\text{Total number of germinated seeds}}{\text{Total number of tested seeds}} \times 100\%$$

Metabolite extraction: The protocol for Gas Chromatography-Mass Spectrometer (GC-MS) metabolite extraction was in accordance with that of previously described procedure (Lisec *et al*., 2006). The collected samples (100 mg) were grinded in a mortar using liquid nitrogen, then transferred into 10 mL centrifuge tubes. After adding 1.4 mL of 100% methanol (precooled at -20°C) and vortexing for 30 s, 60 µL of polar internal standard (0.2 $mg \cdot mL^{-1}$ 1,2-benzenediol in methanol) was added to the tube. The samples were vortexed again for 30 s and placed into an ultrasound machine for 30 min at 40°C, followed by centrifugation for 20 min at 4000 rpm. Then, we transferred the supernatant to a 10 mL centrifuge tube which was followed by addition of 750 µL of chloroform and 1.4 mL of ddH_2O and the mixture was vortexed for 30s prior to centrifugation at 4000 rpm for 20 min. The supernatant was transferred into a new tube and blow-dried with nitrogen. Subsequently, 60 µL of methoxypyridine (20 $mg \cdot mL^{-1}$) was added and vortexed for 30 s. After a reaction time of 2 h at 37°C, 60 µL of N,O-bis(trimethylsilyl) trifluoroacetamide (BSTFA) reagent (containing 1% trimethylchlorosilane) was added to the tube. After reacting for 1.5 h at 37°C, the samples were used for GC-MS analysis.

Metabolite analysis by GC-MS: The GC-MS data were obtained using an Agilent 7890B-5977B (Agilent, Santa Clara, CA, USA) system equipped with an HP-5 MS capillary column (30 m × 0.25 mm, 0.25 µm film thickness, Agilent J & W Scientific, Folsom, CA, USA). Helium was used as a carrier gas at a constant flow rate of 1.0 $mL \cdot min^{-1}$. 1 µL sample volume was injected in split mode at a ratio of 5:1 and at a constant temperature of 280°C. The ion source and interface temperatures were set to 230 and 150 °C, respectively. The initial temperature of the column was 40°C for 5 min, and then after it was increased to 300°C at a rate of 10°C/min and remained constant for 5 min. Mass spectra were taken at 70 eV, and the mass range was from 35 to 780 m/z. The solvent delay was 8.5 min.

Data analysis: To ensure the stability of the assay, we performed six biological repeats and analyzed them under the identical conditions. The QCs were injected at regular intervals throughout the GC-MS analytical run to provide a set of data from which repeatability could be assessed. All the GC-MS data were processed by XCMS (available online: http://www.bioconductor.org) running under the R package (available online: http://www.r-project.org), which produced a matrix of features with the associated retention times, accurate masses, and peak areas. All internal peaks were removed from the data set. The resulting data were normalized to the total peak area of each sample in Excel 2010 (Microsoft, Redmond, WA, USA). Principal component analysis (PCA) and orthogonal partial least squares-discriminant analysis (OPLS-DA) models were generated using Simca-P software version 14.0 (Umetrics AB, Umea, Sweden, Available online: www. umetrics. com/simca). The data scaling modes of PCA and OPLS-DA analyses were unit variance scaling and Pareto scaling, respectively. The differential metabolites were selected on the basis of the combination of the statistically significant threshold of variable influence on projection (VIP) values obtained from the OPLS-DA model and the p-value from a two-tailed Student's t-test of the normalized peak area; metabolites with VIP >1.0 and $p < 0.05$, respectively, were selected. For GC-MS analysis, metabolites were identified by searching the commercial database NIST11 (Vinaixa *et al*., 2016) after their mass spectra were deconvoluted by the Automated Mass Spectral Deconvolution and Identification System (AMDIS) (Meyer *et al*., 2010). Peaks with a similarity index of more than 70% were tentatively identified as metabolites. The identified metabolites were mapped to general biochemical pathways according to their annotation in the Kyoto Encyclopedia of Genes and Genomes (KEGG) database (available online: http://www.kegg.jp/kegg/ pathway.html). Pathway analysis was performed using MetaboAnalyst 4.0 (available online: http://www.metaboanalyst.ca/Metabo Analyst/) (Xia *et al*., 2015). The metabolome data of the differential metabolites were used for this analysis and were subsequently normalized by sum, log-transformed, and Pareto-scaled (Int. J. Mol. Sci. 2018, 19, 728 16 of 19) thereby compared with the KEGG pathway library of *Arabidopsis thaliana*. Metabolite-metabolite correlations between identified metabolites were performed by using the Pearson correlation coefficients. The metabolic network based on the results of the Pearson correlation analysis was constructed by Cytoscape software version 2.8.3 (Cytoscape Consortium, San Diego, CA, USA, Available online: www.cytoscape.org/). The heatmap was generated with R software.

Results

Effects of sand storage on seed germination of *P. cyrtonema*: The germination percentage of *P. cyrtonema* treated with sand storage at room temperature -5~15°C for 30 d was measured (Fig. 1). The seed germination rate after sand storage was significantly (3.69 times) higher than that of the control group. The results showed that sand storage treatment could improve the germination rate of *P. cyrtonema* seeds.

***P. cyrtonema* seeds of germination at different sand storage times:** The seed activity, embryo rate, and germination rate of *P. cyrtonema* seeds were determined at different times after being stored in sand at room temperature -5~15°C (Table 1). The results depicted that

the change in seeds activity was not obvious. With the increase of sand storage time, the embryo rate of *P. cyrtonema* seeds showed an increasing trend which was the highest at 90 d, but the seed activity was decreased at this time. Simultaneously, with the increase of sand storage time, the germination rate of *P. cyrtonema* seeds increased initially with the maximum rate at 60 d which was followed by decrease. Compared with the control group, the germination rates of *P. cyrtonema* seeds treated with sand storage were significantly higher (4.6 times) than those of the control group.

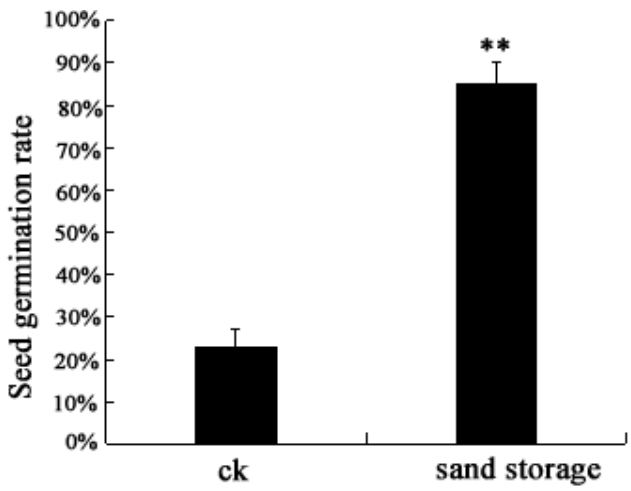

Fig. 1. Effects of sand storage on seed germination of *P. cyrtonema*, extremely significant $^{**}p < 0.01$.

***P. cyrtonema* seeds of germination at different sand storage temperatures:** In this study, the seed activity, embryo rate, and germination percentage of *P. cyrtonema* seeds treated with sand storage at different temperatures for 60 d were measured (Table 2). The embryo rate of *P. cyrtonema* treated with sand storage at -20°C was higher than that of other treatments, but the seed activity was the lowest. At the same time, the seed germination rate of sand storage treatment at 4°C and room temperature -5 to 15°C were significantly (1.66 and 1.88 times, respectively) higher than that obtained at 26°C. The results showed that sand storage at 4°C or room temperature -5 to 15°C were suitable for seeds germination of *P. cyrtonema*. Therefore, the following experiments were carried out using sand storage at 4°C, for the temperature was relatively easy to control.

Metabolic profiling of the seed coat and peeled seeds of *P. cyrtonema* at different storage times: The metabolic profiles of the seed coat and peeled seeds during four sand storage stages were investigated using GC-MS. Total ion chromatograms (TICs) (Fig. 2) showed differences in chromatographic characteristics between different seed organs and sand storage stages. The retention time was reproducible and stable, demonstrating the reliability and validity of metabolomic analysis. Metabolome-wide expression profiling showed the high metabolite expression during sand storage. Through comparative analysis, 85 and 74 metabolites were identified in seed coat and peeled seeds, respectively (Fig. 3). Significant differences in the metabolite profiles existed between the seed coat and peeled seeds. In particular, the metabolites in the seed coat were more active than those in the peeled seeds. Among the metabolites, 65 metabolites were common to both organs, while 20 and 9 metabolites were identified specifically in the seed coat and peeled seeds, respectively (Fig. 3B). The seed coat specific metabolites included four carbohydrates, six alcohols, four organic acids, four nitrogenous , and two others, whereas the nine metabolites specific to peeled seeds included two carbohydrates, five organic acids, and two other metabolites (Fig. 3A).

Table 1. The seed activity, embryo rate and germination percentage of *P. cyrtonema* seeds at different sand storage times.

Sand storage times /d	Seed activity /%	Seed embryo rate /%	Seed germination percentage /%
0	96.0 ± 0.02 a	55.3 ± 0.059 b	20.8 ± 0.053 c
30	97.0 ± 0.026 a	57.7 ± 0.076 b	85.3 ± 0.049 a
60	97.3 ± 0.025 a	62.7 ± 0.059 ab	94.7 ± 0.015 a
90	82.0 ± 0.082 b	63.9 ± 0.079 a	77.0 ± 0.02 b

Note: a , b and c are multiple comparative alphabetic markers; the same letter indicates no significant difference at the significance level of $p<0.05$

Table 2. The seed activity, embryo rate and germination percentage of *P. cyrtonema* seeds at different sand storage temperatures.

Sand storage temperatures / °C	Seed activity / %	Seed embryo rate / %	Seed germination percentage / %
-20	63.0 ± 0.006 c	63.8 ± 0.032 a	49.3 ± 0.04 c
4	93.0 ± 0.009 ab	61.7 ± 0.081 ab	83.3 ± 0.038 b
-5~15	97.3 ± 0.015 a	62.7 ± 0.059 a	94.6 ± 0.012 a
26	84.0 ± 0.012 b	59.1 ± 0.049 b	50.3 ± 0.028 c

Note: a, b and c are multiple comparative alphabetic markers; the same letter indicates no significant difference at the significance level of $p<0.05$

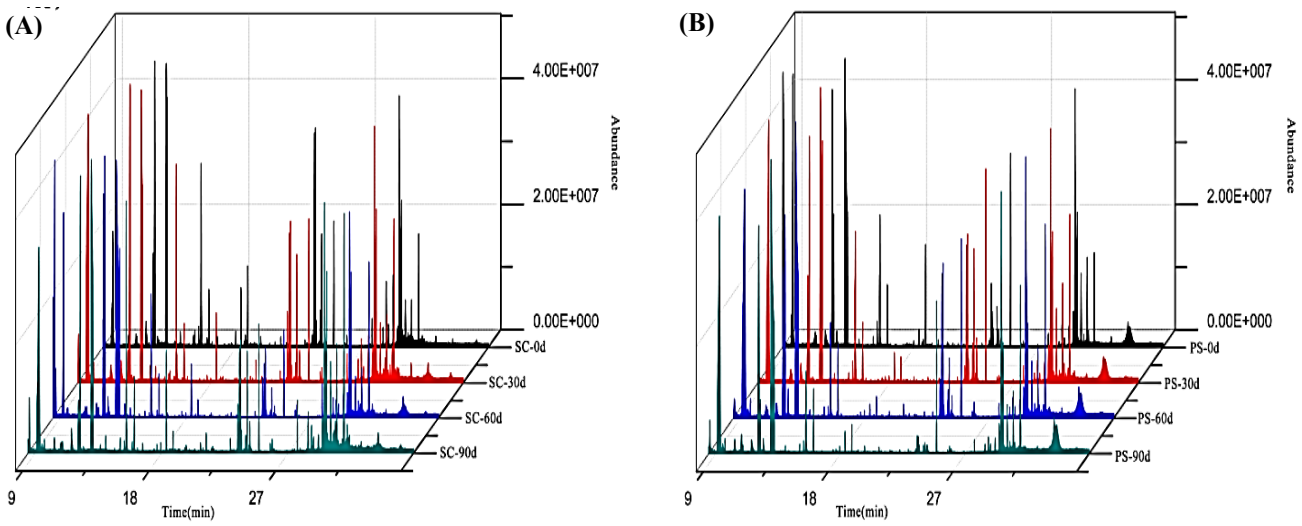

Fig. 2. Overlays of total ion chromatograms (TICs) by GC-MS analysis of seed coat and peeled seeds under different sand storage times. (A). Overlays of total ion chromatograms (TICs) of seed coat (SC). (B). Overlays of total ion chromatograms (TICs) of peeled seeds (PS).

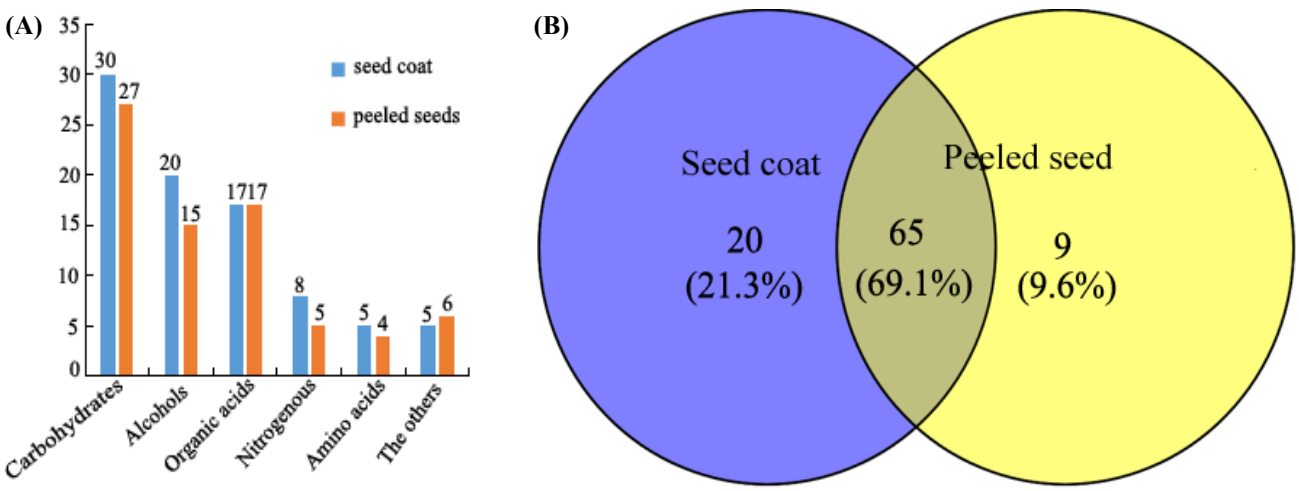

Fig. 3. Distribution of the identified metabolites in the storage seed. (A) Functional classification of significantly different metabolites in the seed coat and peeled seeds. (B) Venn diagram showing the distribution of the significantly different metabolites in the seed coat and peeled seeds.

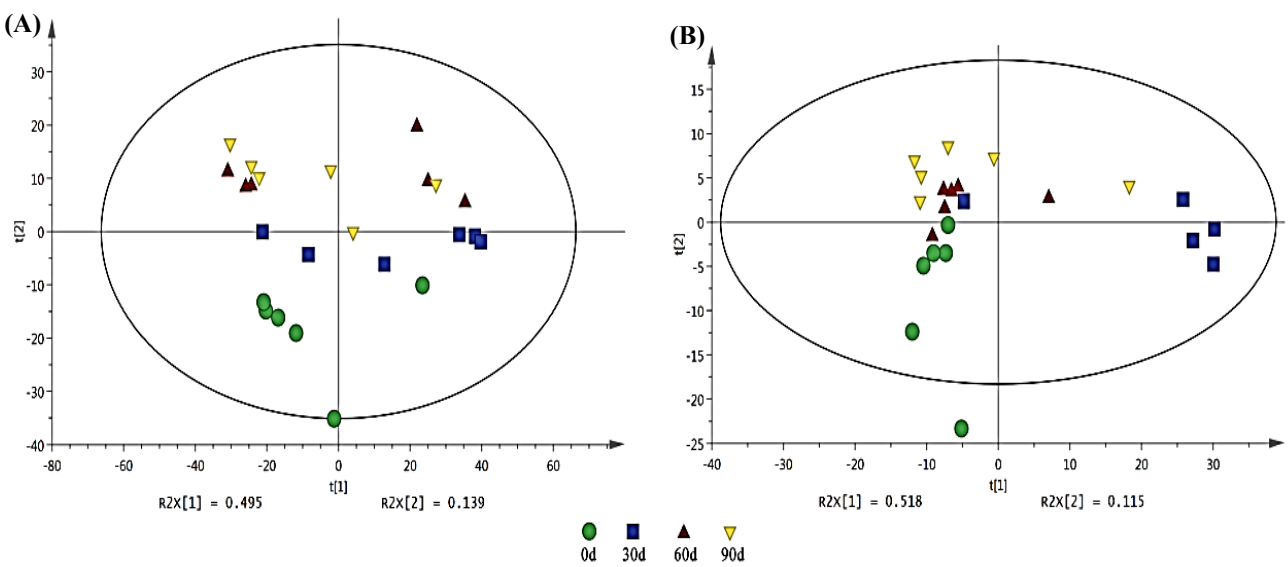

Fig. 4. Principal component analysis (PCA) of identified metabolites. Time periods include 0 d (non-sand storage), 30 d, 60 d, and 90 d. (A). PCA of seed coat metabolite profiles during seed sand storage. (B). PCA of peeled seeds metabolite profiles during seed sand storage.

Principal component analysis (PCA) of metabolites: PCA was carried out using the unsupervised projection method to detect the metabolite distribution at four storage times in the seed coat and peeled seeds. As shown in Fig. 4A, the metabolites in seed coat were analyzed. The first principal component for seed coat covered 49.5% of the variability, and the second principal component covered 13.9%. According to the dispersion trend of the sample score plot, the metabolites in seed coat varied significantly during sand storage, but the metabolites in seed coat did not differ significantly when stored in sand for 60 d vs. 90 d. As shown in Fig. 4B, the first principal component for peeled seeds covered 51.8% of the variability, and the second principal component covered 11.5%. According to the dispersion trend of the sample score plot, the metabolites in peeled seeds varied significantly during sand storage, but sand storage for 30 d could be clearly distinguished from other three periods.

Analysis of differential metabolites in the seed coat of *P. cyrtonema* seeds at different sand storage times: The OPLS-DA was further employed to identify the metabolites in the seed coat of *P. cyrtonema* at different sand storage times (VIP>1.0, p<0.05). Sixteen metabolites that showed significant changes and greatly contributed to typing from 0 d vs. 30 d were screened (Fig. 5A). Out of sixteen, ten metabolites were screened and identified. Among them, four metabolites were significantly upregulated, and six were significantly downregulated. The upregulated and downregulated metabolites are listed in Fig. 6A. The metabolites mainly involved glycolysis, TCA cycle, galactose metabolism, and amino acid metabolism, such as pyruvate, GABA, myo-inositol and benzoate. Twelve metabolites that showed significant changes and greatly contributed to typing from 30 d vs. 60 d were screened (Fig. 5B). Out of twelve, eight metabolites were screened and identified, and all these metabolites were significantly down regulated. These metabolites included carbohydrates, alcohols, and acids which were mainly involved in glycolysis and galactose metabolism, such as sorbitol, phosphate and sorbose (Fig. 6B). Five metabolites that showed significant changes and greatly contributed to typing from 60 d vs. 90 d were screened (Fig. 5C). Among them, two metabolites were screened and identified. One metabolite was upregulated, while other was downregulated (Fig. 6C). Lactulose and myo-inositol were metabolites common to the 0 d vs. 30 d and the 30 d vs. 60 d comparisons, and they changed in different manner when compared to each other. Pyruvate was found in the 0 d vs. 30 d and the 60 d vs. 90 d comparisons, and it changed in opposite directions between the two. These results showed that the TCA cycle of *P. cyrtonema* seeds was affected by sand storage times.

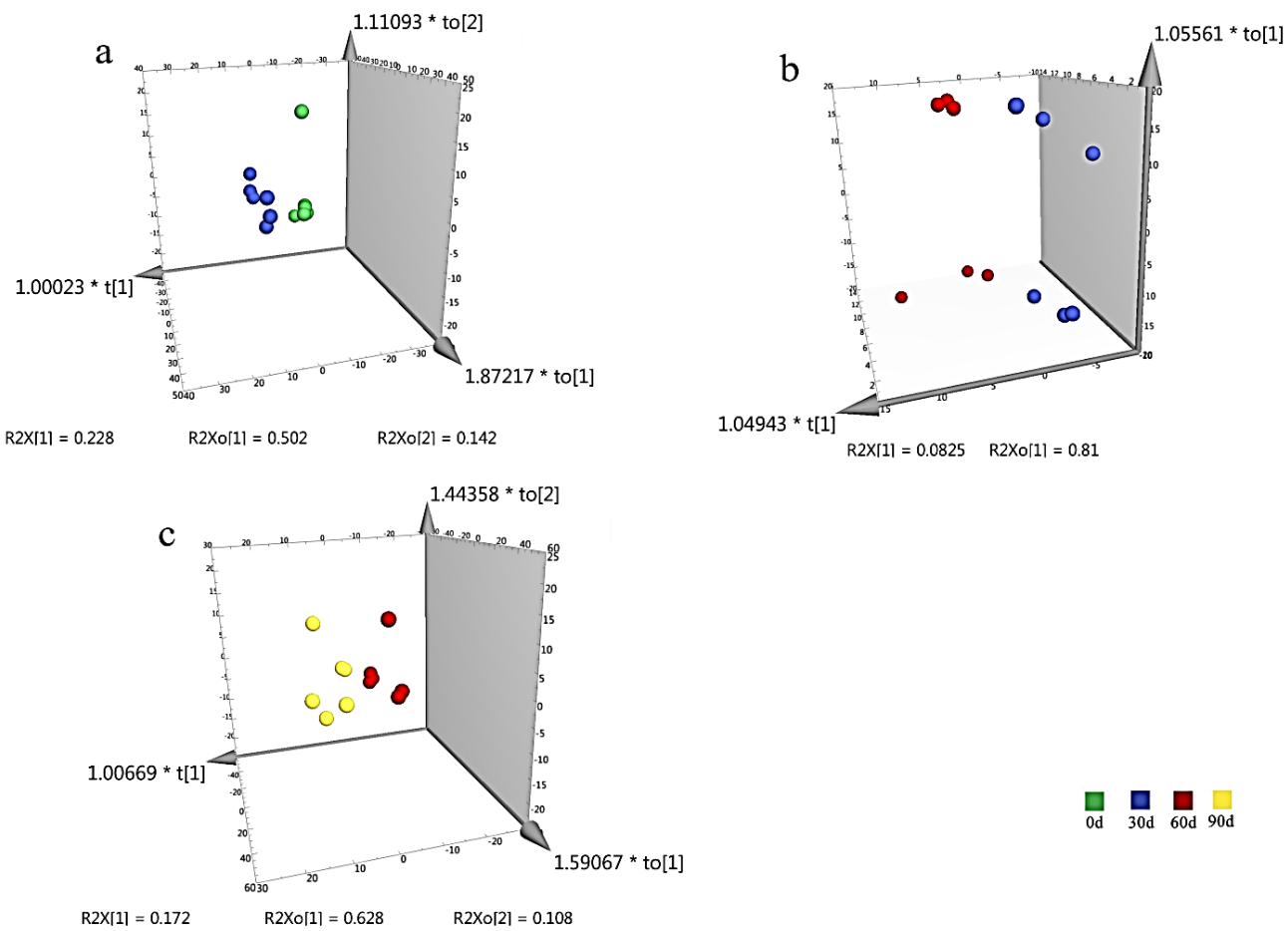

Fig. 5. The OPLS-DA score map of metabolites in *P. cyrtonema* seed coat at different sand storage times. (A). The OPLS-DA score map of metabolites from 0 d to 30 d. (B). The OPLS-DA score map of metabolites from 30 d to 60 d. (C). The OPLS-DA score map of metabolites from 60 d to 90 d.

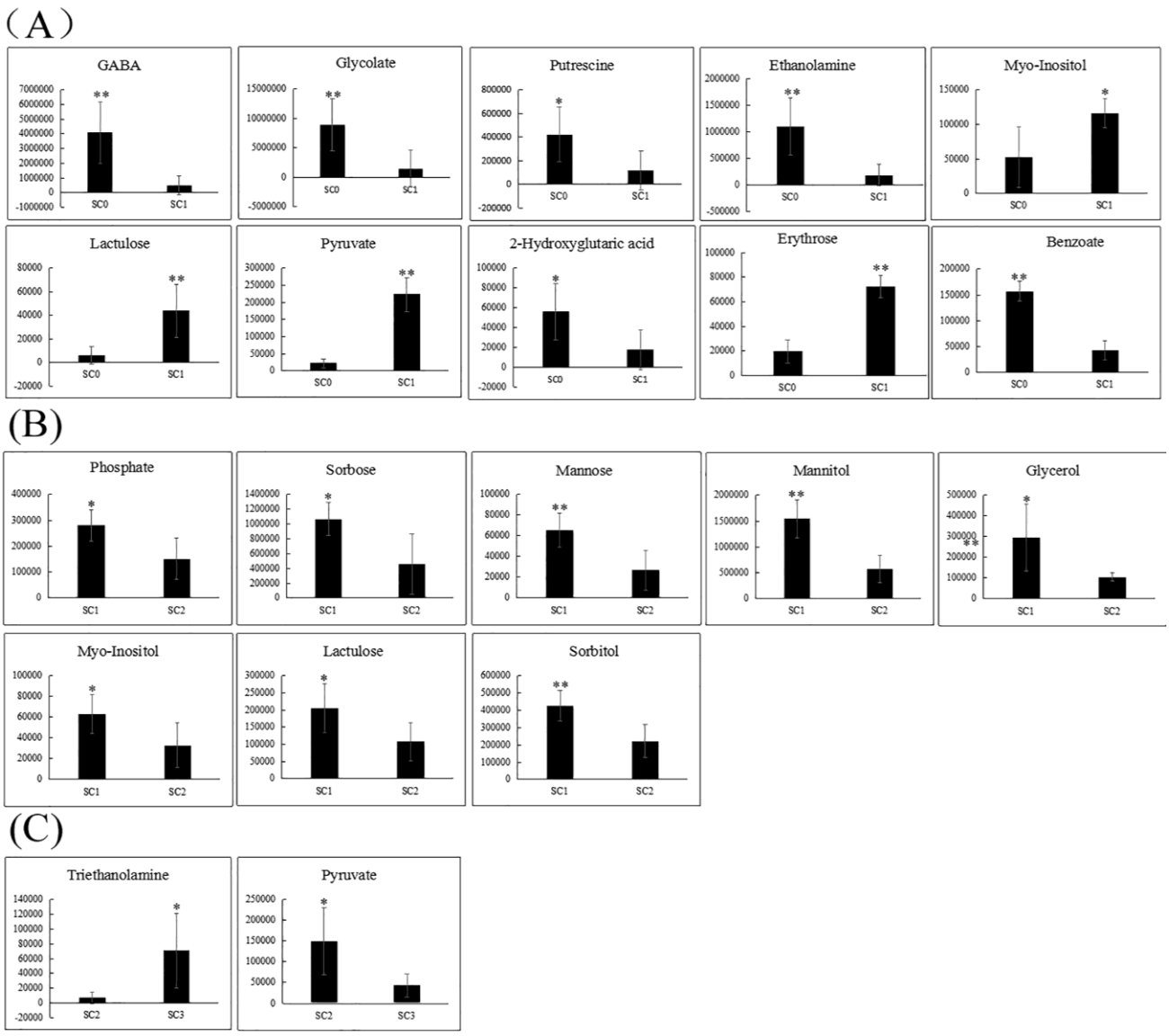

Fig. 6. Differential metabolites in seed coat of *P. cyrtonema* seeds during different sand storage times. Longitudinal coordinate is the peak area of metabolites. (A). The differential metabolites from 0 d to 30 d. (B). The differential metabolites from 30 d to 60 d. (C). The differential metabolites from 60 d to 90 d. Significant *p< 0.05, extremely significant **p< 0.01.

Analysis of differential metabolites in peeled seeds of *P. cyrtonema* at different sand storage times: We further employed OPLS-DA to identify the metabolites in peeled seeds of *P. cyrtonema* at different sand storage times (VIP>1.0, p<0.05) (Fig. 7). Seven metabolites that showed significant changes and greatly contributed to typing from 0 d vs. 30 d were screened (Fig. 7A), and two metabolites (myo-inositol and sorbose) were upregulated with their involvement in glycolysis and galactose metabolism, respectively (Fig. 8A). Twelve metabolites that showed significant changes and greatly contributed to typing from 30 d vs. 60 d were screened (Fig. 7B), and six metabolites (mainly acids and carbohydrates, such as malate, succinate and GABA) all of which were significantly upregulated (Fig. 8B) with their role in the TCA cycle and amino acid metabolism. Ten metabolites that showed significant changes and greatly contributed to typing from 60 d vs. 90 d were screened (Fig. 7C), and nine metabolites (acids, carbohydrates and alcohols, such as malate, succinate, sorbose, and sorbitol) (Fig. 8C) were downregulated. Malate and succinate were the common metabolites in the 30 d vs. 60 d and the 60 d vs. 90 d comparisons, and they also changed in opposite directions (Fig. 8), which demonstrated that metabolites were changed greatly in order to provide energy to put an end to seed dormancy during sand storage.

Dynamic metabolic changes of the seed coat and peeled seeds during sand storage: All metabolite data from seed coat and peeled seeds were analyzed by HCA to reveal the global coordinate changes in the metabolites during sand storage (Fig. 9). The expression of metabolites in the seed coat could be classified into four clusters (Fig. 9A). Cluster 1 included ten carbohydrates, two alcohols, two acids (malate and hexadecanoic acid), one amino acid (beta-alanine), one nitrogen-containing metabolite and one other compound. These metabolites increased gradually during sand storage. Such as malate, it is an important intermediate of the TCA cycle, indicating that sand storage promoted the TCA cycle in

seed coat. Cluster 2 included most alcohols, nine organic acids, four amino acids, six nitrogen-containing compounds and five carbohydrates. The metabolites were downregulated during sand storage. These metabolites were involved in glycolysis and other pathways. The decrease of these metabolites indicated that they were used to provide energy during sand storage. Cluster 3 included five carbohydrates (levoglucosan, rhamnose, sucrose, maltose, d-glucose), and these metabolites were upregulated from 0 d to 60 d and then downregulated significantly at 90 d of sand storage, indicating that 60 d of sand storage was the switch point. Cluster 4 mainly included four carbohydrates, six alcohols and seven organic acids. These metabolites were upregulated significantly in sand storage, and the data indicated that 30 d of sand storage was a switch point for them.

The metabolites in the peeled seeds could be classified into five clusters (Fig. 9B). Cluster 1 included four carbohydrates (turanose, trehalose, 2-O-glycerol-alpha-d-galactopyranoside, gulose), two alcohols (muco-inositol, myo-inositol) and two phenylalkanes (benzene, propyl-, 1-methylethyl-benzene). These metabolites increased markedly at 30 d of sand storage and then decreased markedly at 60 d, which indicated that they changed significantly at 60 d of sand storage. Cluster 2 mainly included four alcohols (1,5-anhydro-D-sorbitol, glycerol, scyllo-inositol, 2,4-dimethylphenol), five carbohydrates (lactulose, alpha-D-lyxopyranose, 3-alpha-mannobiose, maltose and cellobiose), and two acids (hexadecanoic acid and gluconic acid), which increased significantly in 30 d of sand storage, and maintained upto 60 d. But the decreases at 90 d were significant, which indicated that sand storage for 30 d and 60 d were turning points. Cluster 3 mainly included organic acids and amino acids, such as malate, succinate, and beta-alanine, which increased significantly in 60 d of sand storage and were significantly higher than the other three periods, suggesting 60 d of sand storage was a turning point. Cluster 4 consisted of three carbohydrates (levoglucosan, beta-D-glucopyranose and erythrose), two amino acids (pyroglutamic acid and GABA), four acids (gluconate, beta-resorcylic acid, 3-hydroxybutyric acid and 4-hydroxybutanoic acid), and three alcohols (threitol, butane-1, 2, 3-triol and erythritol). These compounds decreased gradually in the sand storage process. Metabolites in cluster 5 had similar trends to those in cluster 1, suggesting that 30 d and 60 d of sand storage were turning points.

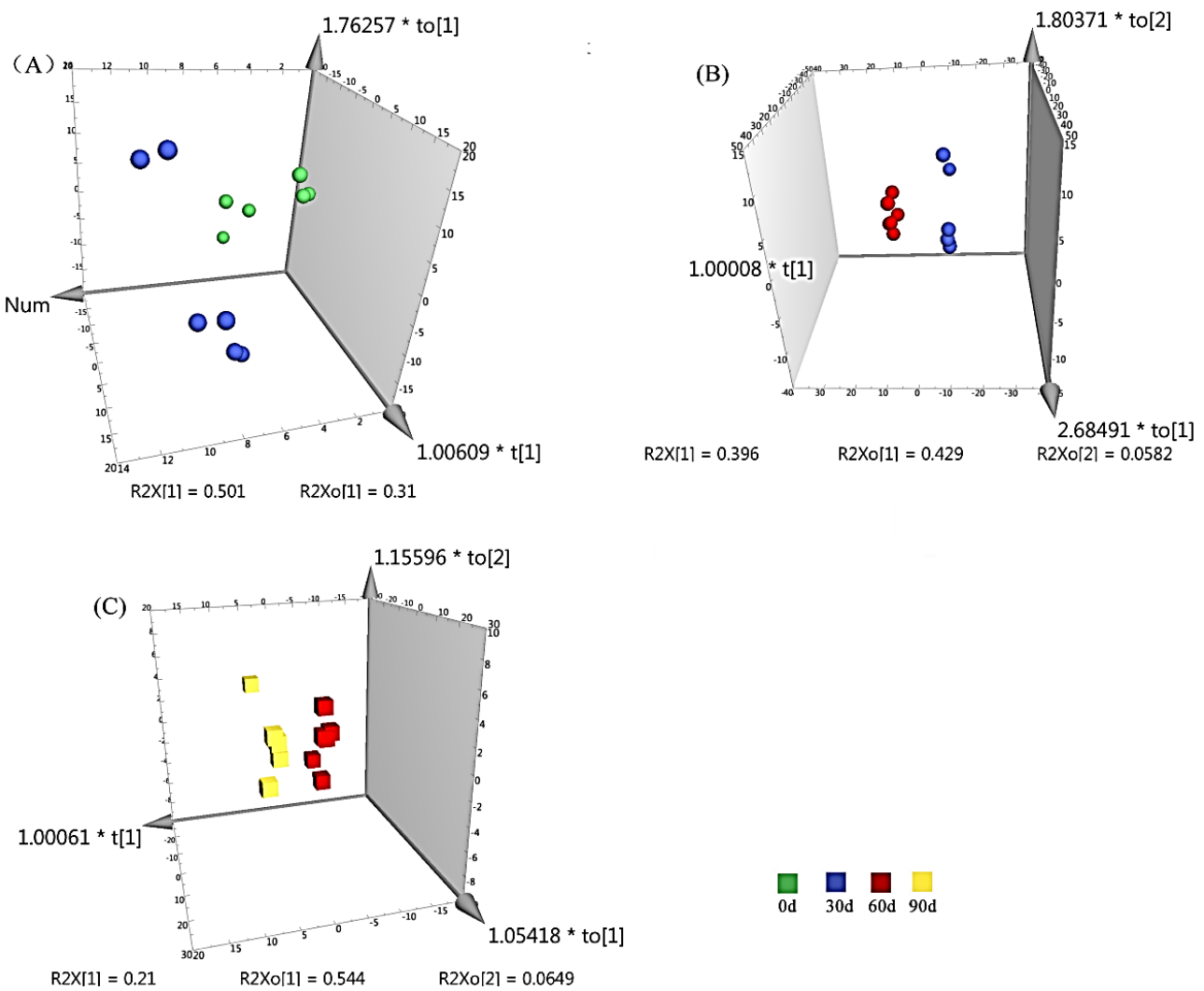

Fig. 7. The OPLS-DA score map of metabolites in *P. cyrtonema* peeled seeds at different sand storage time. (A). The OPLS-DA score map of metabolites from 0 d to 30 d. (B). The OPLS-DA score map of metabolites from 30 d to 60 d. (C). The OPLS-DA score map of metabolites from 60 d to 90 d.

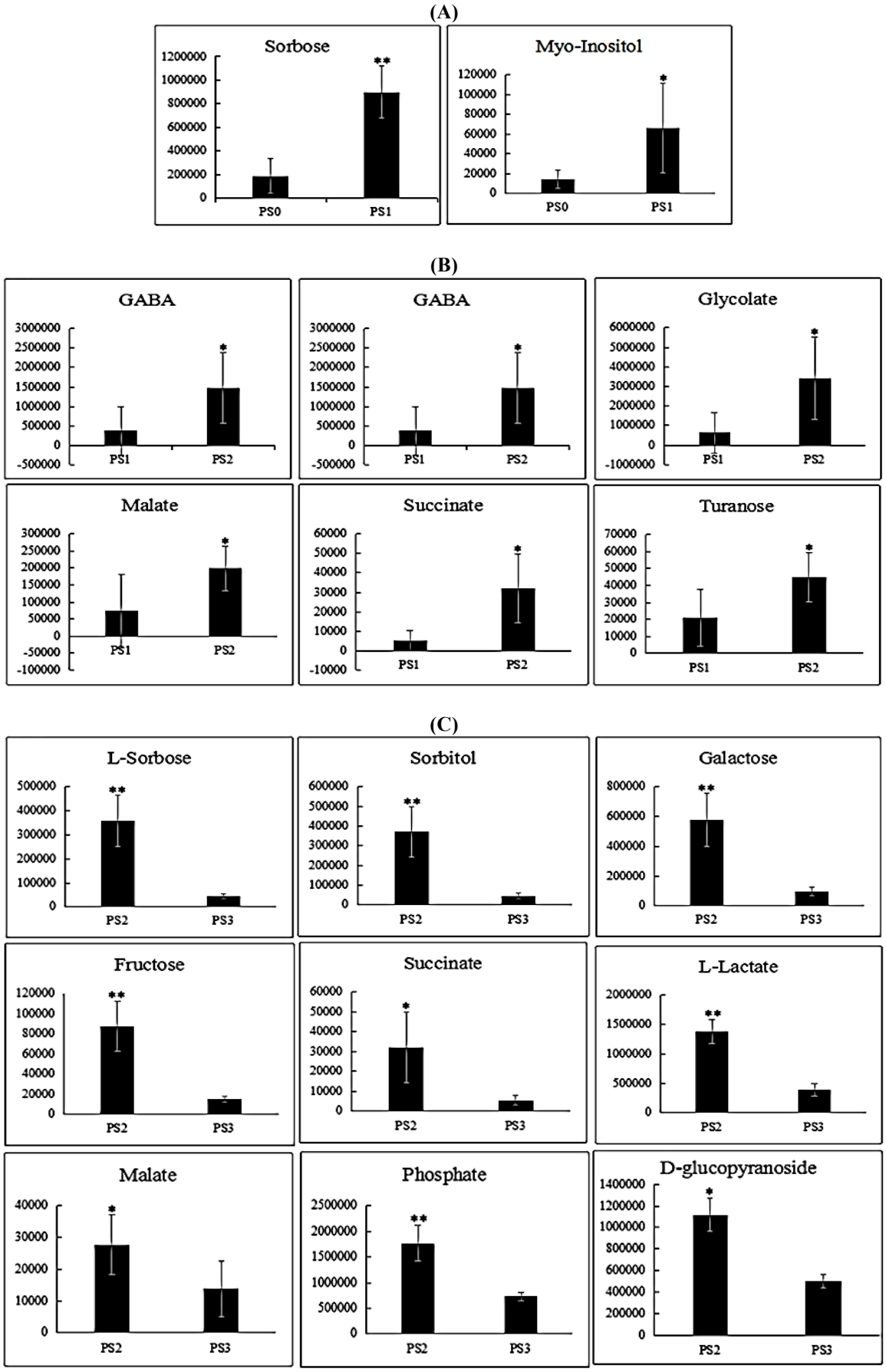

Fig. 8. Differential metabolites in peeled seeds of *P. cyrtonema* during different sand storage times. Longitudinal coordinate is the peak area of metabolites. (A). The differential metabolites from 0 d to 30 d. (B). Differential metabolites from 30 d to 60 d. (C). The differential metabolites from 60 d to 90 d.

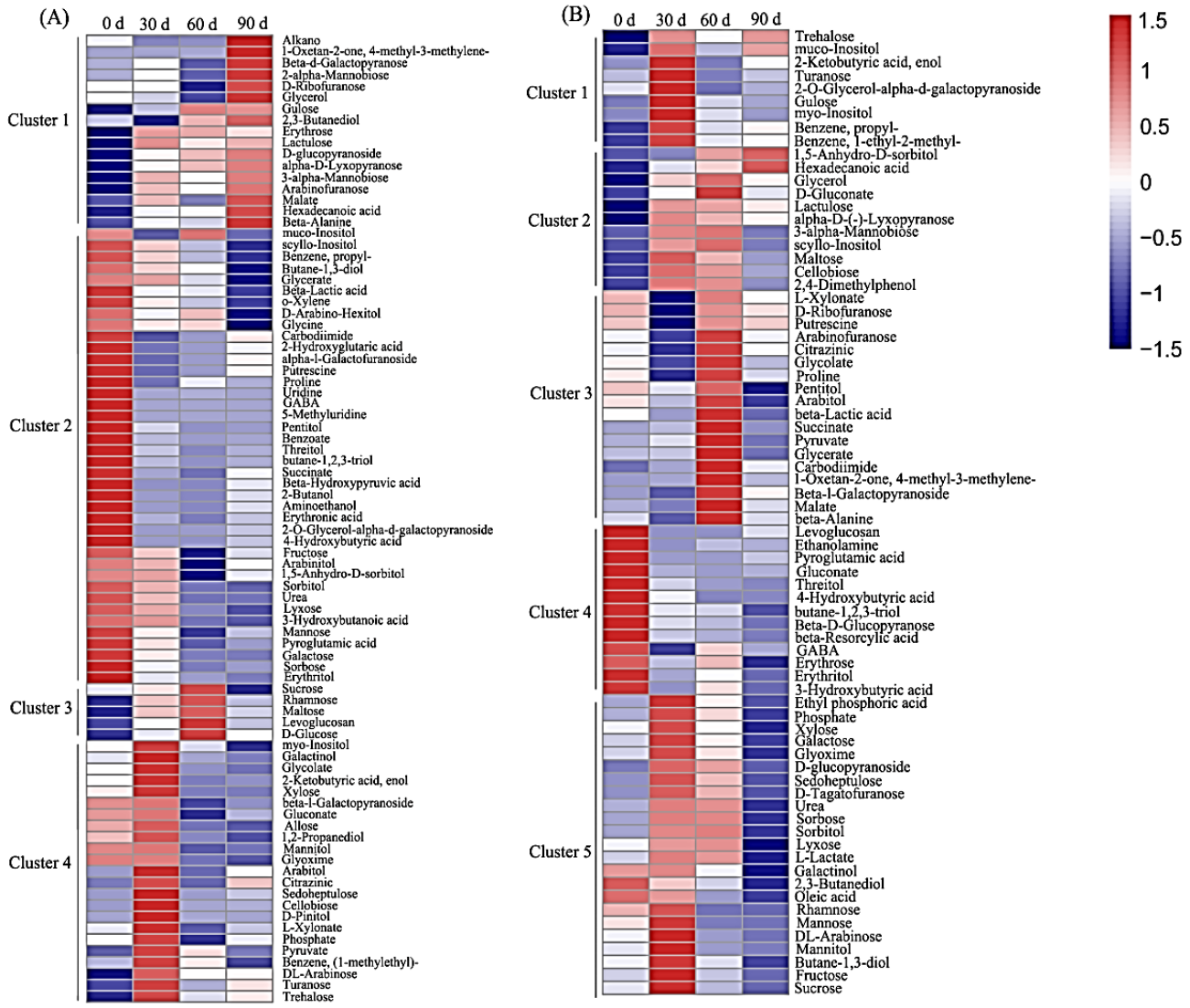

Fig. 9. Hierarchical cluster analysis (HCA) showing the coordinated changes in metabolites during sand storage. The deeper the red color, the higher the content; the deeper the blue color, the lower the content. (A). HCA of the seed coat. (B). HCA of peeled seeds.

Metabolite-metabolite correlation analysis in seed coat and peeled seeds of *P. cyrtonema*: To investigate the relationship between the metabolites, we performed pairwise correlations. Of these pairwise correlations, 75 and 65 significant correlations ($|r| \geq 0.8$ and $p \leq 0.01$) were identified in the seed coat and in the peeled seeds, respectively, during sand storage (Fig. 10). Only one pair showed a significant negative correlation in the peeled seeds, and there were no negative significant correlations in the seed coat.

In the seed coat, seventy-five pairs of metabolites were significantly positively correlated (Fig. 10A), 12 sugars and glycosides accounted for 45.3% of the total significant correlations. For example, lpha-l-Galactofuranoside and succinate (r =0.878, *p* =1.75041E-08), ethanolamine (r =0.856, *p* =9.95567449030475E-08), GABA(r =0.828, *p* =6.00925E-07) was a significant positive correlation. Ethanolamine can synthesize acetic acid and then acetyl-CoA for the TCA cycle. GABA and pentitol (r = 0.932, *p*= 3.88156 E-11), 2-butanol (r = 0.834, *p* = 4.13828E-07), ethanolamine (r = 0.834, *p* = 4.13828E-07), and 2-hydroxyglutaric acid (r = 0.859, *p* = 7.68037E-08) also showed significant correlations. According to the above metabolite correlation data, amino acid metabolism was correlated with alcohol metabolism and the TCA cycle.

In peeled seeds, sixty-four pairs of metabolites were significantly positively correlated, and one pair was significantly negatively correlated (Fig. 10B). 13 sugars and glycosides accounted for 72% of the total significant correlations, of which turanose was negatively correlated with l-xylonate (r = -0.805, *p*=2.07119E-06), but positively correlated with sucrose (r = 0.827, p = 6.10337199726637E-07), dl-arabinose (r = 0.907, *p* = 9.64868146323696E-10), mannitol (r = 0.84, *p* = 2.90812882925093E-07), myo-inositol (r= 0.87, *p*= 3.4770622284719E-08). In addition, malate was positively correlated with beta-alanine (r = 0.838, *p* = 7.68037E-07), glyceric acid (r = 0.812, *p* = 1.46048E-06), succinic acid was also positively correlated with glyceric acid (r = 0.893, *p* = 4.56865878711614E-09), which indicated that the TCA cycle was positively correlated with amino acid and pentose phosphoric acid metabolism pathways.

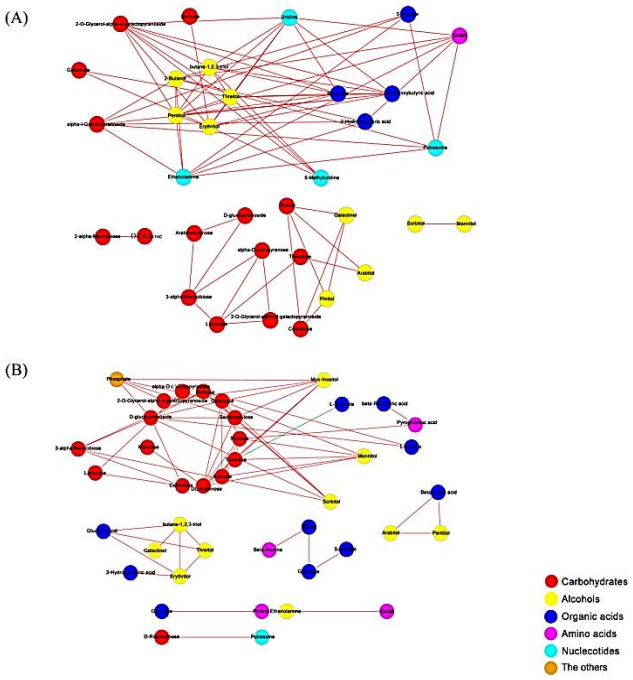

Fig. 10. Metabolite network based on significant correlations (|r|≥ 0.8 and p≤0.01). Nodes represented metabolites, and edges represented metabolite relationships. Different node colors indicated metabolites in different pathways. Red edges showed positive correlations, and green edges showed negative correlations. (A). corresponded to metabolite-metabolite significant correlations of the seed coat. (B). corresponded to metabolite-metabolite significant correlations of the peeled seeds.

Changes of metabolites in seed coat and peeled seeds of *P. cyrtonema* in metabolic pathways: Our study sought to obtain a more detailed overview of the abundance of similarities and/or differences of the identified substances in each storage time of both organs (Fig. 11). In starch and sucrose metabolism, trehalose showed a similar trend in seed coat and peeled seeds during sand storage. Trehalose increased at 30 d of sand storage, decreased significantly at 60 d and slightly increased at 90 d. The sucrose, fructose, and maltose in peeled seeds were significantly higher than those in other periods when stored in sand for 30 d, indicating that these compounds were fully utilized and entered the next metabolic pathway after 30 d of sand storage. The sucrose and maltose in seed coat decreased significantly after 60 d of sand storage. In the TCA cycle , seed coat and peeled seeds had the same metabolites, but the trend of metabolites in seed coat and peeled seeds was different. During sand storage, pyruvate, succinate, and malate in peeled seeds showed similar trends, and the metabolites were significantly higher than those in the other three periods at 60 d of sand storage, indicating that the TCA cycle was relatively active at this time. Succinate in seed coat showed a significant downward trend in the sand storage process and increased slightly at 90 d. The pyruvate in seed coat was significantly higher than that in other three periods during 30 d of sand storage. Malate in seed coat and in peeled seeds changed in opposite directions.

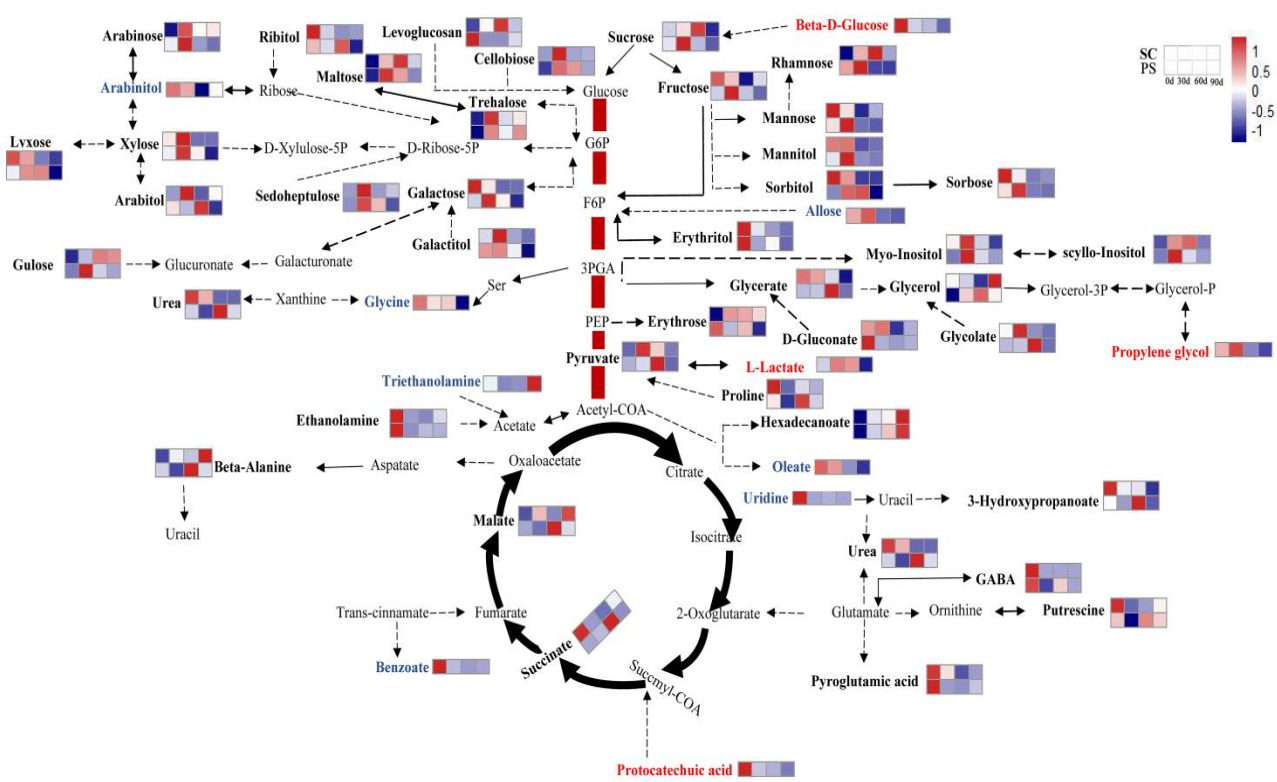

Fig. 11. Primary metabolism pathways of measured metabolites in seed coat (SC) and peeled seeds (PS). Represented pathways are simplified versions of the tricarboxylic acid cycle (TCA), glycolysis, amino acid synthesis, and sucrose synthesis. Within each box, rows represent organs (*upper row*: SC; *lower row*: PS). Each column is a sand storage stage (*from left to right*: non-sand storage, ck (0d); 30 d; 60 d; 90 d), as shown in the upper right corner. Average metabolite intensity is color-coded according to the scale in the upper right corner. Metabolites measured in seed coat and peeled seed, non-measured, only measured in seed coat, only measured in peeled seed are displayed in black thickening, gray, blue and red font respectively (color Fig. online).

The analysis of amino acids showed that the changing trends in seed coat and peeled seeds were different. For example, the beta-alanine in seed coat was upregulated at 30 d and downregulated at 60 d, and then it increased significantly at 90 d to a level significantly higher than that in the other three periods. However, the change of beta-alanine in the peeled seeds was opposite, being higher than that in the other three periods in peeled seeds at 60 d. In the process of sand storage, the proline in the seed coat and peeled seeds showed similar change trends, besides some differences. The proline in seed coat at 0 d was significantly higher than that in the other three periods, while, it was significantly higher at 60 d than at the other time points in peeled seeds. On the other hand, glycine was detected only in the seed coat.

Discussion

The *Pinellia ternata* seeds at 4°C sand storage was conducive for improving the vigor and germination ability of the seeds (Ma *et al*., 2020). The germination rate of seeds stored in low-temperature sand was higher than that stored in normal-temperature sand (Peng *et al*., 2016). It was found that sand storage could significantly improve the germination rate of *P. cyrtonema* seeds, which was consistent with the results of Wang Zhanhong *et al*. (Wang *et al*., 2012). The most significant reason was that low-temperature sand storage can increase the activity of enzymes, promote the expression of related genes, and the degradation of macromolecule substances in seeds, and provide a material basis for seed germination. Since both the sand storage at 4°C and -5 to 15°C were suitable for seeds germination of *P. cyrtonema*, sand storage at room temperature -5 to 15°C for seed production in winter can be selected to save the production cost with easy operation.

The main reserves can be rapidly mobilized and enzymatically broken down to simpler components, such as glucose, amino acids, glycerol, and fatty acids, in some seeds. These hydrolysis products were transferred to embryos, where they provided an energy source and materials for seed germination (Bewley & Black, 1994). Maltose is decomposed into glucose from the degradation of starch production, and then, it participates in glycolysis. Our results showed that maltose was upregulated in peeled seeds stored in sand for 30 d and decreased gradually in sand storage from 60 d to 90 d. Maltose in seed coat increased when stored in sand for 30–60 d (Fig. 9A). The products of starch mobilization were transported through the scutellum parenchyma to the scutellum vasculature, which connects to phloem for embryonic axis growth when starch degradation begins in the endosperm (Humphreys, 1987). Sugars could be derived from gluconeogenesis and the degradation of polysaccharides (Guo *et al*., 2015). In this study, most of the polysaccharides in peeled seeds, such as galactose, galactitol, cellobiose and mannitol, decreased significantly after 30 d of sand storage. Levoglucosan, gluconic acid and trehalose all decreased significantly after sand storage. This suggested that the initial monosaccharides were originated from the degradation of polysaccharides and other pathways of carbon metabolism in the peeled seeds. Changes in these carbohydrates during sand storage might provide energy for seed germination. These changes in sugars could act as osmolytes, might enhance water movement toward the seed germination (De Faÿ *et al*., 2000) and provide power for seed germination.

Myo-inositol is related to many aspects of plant physiology, such as carbohydrate metabolism, seed germination, stress response, and cell wall formation (Loewus & Loewus, 1983; Omar *et al*., 2021). Myo-inositol could be converted into phytic acid, the most abundant form of phosphate in seeds (Loewus & Murthy, 2000; Nunes *et al*., 2006). Myo-inositol in the seed coat and peeled seeds was significantly higher at 30 d than in the other three periods (Fig. 9). These results showed that myo-inositol was transformed after sand storage, which provided conditions for seed germination.

Owing to limited oxygen permeation into dense seed tissues, the amount of energy required to fuel seed development seems to depend mainly on glycolysis (Yang *et al*., 2007). Sugars play an important role in providing energy in the glycolysis pathway. Based on our results, fructose increased at 30 d of sand storage, which was significantly higher than that in peeled seeds. In the other three periods, fructose in seed coat showed a downward trend during sand storage (Fig. 9A). This supported previous studies showing that the energy demand for seed germination was provided mainly through glycolysis. Decrease in the concentration of fructose and galactose during cold stratification might be involved in the energy supply for cell division (Omar *et al.*, 2021). Therefore, it can be speculated that the biosynthesis of new compounds and other energy metabolism needs are provided by glycolysis in peeled seeds.

The TCA cycle is a common pathway for the complete oxidation and decomposition of sugar, protein and fat, as well as a pivot of energy metabolism. In this study, the content of one organic acid, pyruvate, in peeled seeds was significantly higher than that in other three periods at 60 d of sand storage (Fig. 9B). Furthermore, the contents of malate and succinate were significantly improved. At this time, the germination rate of seeds was also higher which implied that the TCA cycle was active in peeled seeds stored in sand for 60 d to prepare energy for seed germination.

Amino acids not only play a role as precursors of protein synthesis but also maintain osmotic potential as compatible solutes, which can be decomposed into other products and enter the TCA cycle to generate energy (Church *et al*., 2020; Joshi *et al*., 2021). GABA is associated with seed energy production (Li *et al*., 2021), and regulates plant development in response to oxidative stress. GABA in peeled seeds was downregulated significantly after 30 d of sand storage and increased significantly at 60 d. The increase in GABA indicated its strong protective effect on oxidative stress and provided energy for seed germination.

In summary, the current and previous findings showed that sand storage had different effects on different parts of seeds (Bian *et al*., 2018). Our results confirmed that sand storage could provide an energy source and materials for seed germination through regulating

metabolites of the seed coat and peeled seeds, thus break the dormancy of *P. cyrtonema* seeds and improve the germination rate. In the future, we use physiological and biochemical experiments to detect the changes of physiological indicators during sand storage of *P. cyrtonema* seeds in order to explore the mechanism of sand storage deeply. Also it would be worthwhile to identify the functional genes or transcription factors involved in breaking seed germination of *P. cyrtonema*.

Conclusion

The beneficial effects of sand storage on alleviating the seed dormancy and promoting seed germination of many species, including *P. cyrtonema* are well recognized. Sand storage at 4°C or room temperature -5 to 15°C was suitable for seeds germination of *P. cyrtonema*. In order to study the dynamic changes in metabolites of seed coat and peeled seeds of *P. cyrtonema* at different sand storage times, metabonomics approach was used. The changes in metabolites in peeled seeds were more complex than those in seed coats. In the process of sand storage, 30 d and 60 d of sand storage showed noticeable effects, which involved multiple metabolic pathways. Starch, as the main energy storage material of seeds, and degraded small-molecule compounds entered glycolysis and the TCA cycle during sand storage. Monosaccharides in the seed coat and peeled seeds mainly originated from the hydrolysis of polysaccharides and served as energy sources for seed germination through glycogenesis. At the same time, GABA and myo-inositol were related to seed germination, which could provide conditions for seed germination through different ways. To summarize metabonomics data could provide a more comprehensive and holistic view in exploring the mechanism of ending seed dormancy.

Acknowledgments

The work was supported by the 2018 of Natural Science Research Project of Education Department (Project number 03087060), the Cultivation Technology of Seedlings of Rhizoma *Polygonatum* in Jiuhua, Chizhou (Project number 11006232), and the 2018 National College Students' Innovation and Entrepreneurship Training Program (Project number 201810364032).

Reference

Abo-Hamad, E. H. 2021. Improvement of the growth and some metabolic components of zea mays and helinthus annuus by pre-sowing seed treatments. *Pak. J. Bot*., 53(2):

Bewley, J. and M. Black. 1994. Seeds: Physiology of development and germination. *Plenum. Press*., 67-73.

Bian, F., J. Su, W. Liu and S. Li. 2018. Dormancy release and germination of Taxus yunnanensis seeds during wet sand storage. *Sci Rep*., 8(1): 3205.

Chen, D.L., X. Luo, Z. Yuan, M. Bai and X. Hu. 2020. Seed dormancy release of Halenia elliptica in response to stratification temperature, duration and soil moisture content. *BMC Plant Biol*., 20(1): 352.

Chen, J.Z., X. Huang, X. Xiao, J. Liu, X. Liao, Q. Sun, L. Peng and L. Zhang. 2022. Seed dormancy release and germination requirements of cinnamomum migao, an endangered and rare woody plant in Southwest China. *Front Plant Sci*., 27(13): 770940.

Church, D.D., K. Hirsch, S. Park, I. Kim, J. Gwin, S. Pasiakos, R. Wolfe and A. Ferrando. 2020. Essential amino acids and protein synthesis: insights into maximizing the muscle and whole-body response to feeding. *Nutrients*, 12(12): 3717.

De Faÿ, E., V. Vacher and F. Humbert. 2000. Water-related phenomena in winter buds and twigs of *Picea abies* L. (Karst.) until bud-burst: a biological, histological and NMR study. *Ann. Bot*., 86: 1097-1107.

Guo, R., Z. Yang, F. Li, C. Yan, X. Zhong, Q. Liu, X. Xia, H. Li and L. Zhao. 2015. Comparative metabolic responses and adaptive strategies of wheat (*Triticum aestivum*) to salt and alkali stress. *BMC Plant Biol*., 15: 170.

Han, C.X., S. Zhen, G. Zhu, Y. Bian and Y. Yan. 2017. Comparative metabolome analysis of wheat embryo and endosperm reveals the dynamic changes of metabolites during seed germination. *Plant Physiol. Biochem*., 115: 320-27.

Humphreys, T.E. 1987. Sucrose efflux and export from the maize scutellum. *Plant Cell Environ*., 10: 259-266.

Jin, Q., C. Jiao, S. Sun, C. Song, Y. Cai, Y. Lin, H. Fan and Y. Zhu. 2016. Metabolic analysis of medicinal *Dendrobium officinale* and *Dendrobium huoshanense* during different growth years. *Plos One*., 11.

Joshi, V., P. Nimmakayala, Q. Song, V. Abburi, P. Natarajan, A. Levi, K. Crosby and U. Reddy. 2021. Genome-wide association study and population structure analysis of seed-bound amino acids and total protein in watermelon. *Peer J*., 19;9:e12343.

Kosa, S. and O. Karaguzel. 2020. Effects of seed age, germination temperature, gibberellic acid and stratification on germination of silene compacta. *Pak. J. Bot.*, 52(3):

Li, L., N. Dou, H. Zhang and C. Wu. 2021. The versatile GABA in plants. *Plant Signal Behav*., 16(3): 1862565.

Lisec, J., N. Schauer, J. Kopka, L. Willmitzer and A. Fernie. 2006. Gas chromatography mass spectrometry-based metabolite profiling in plants. *Nat. Protoc*., 1: 387-396.

Loewus, F. A. and P. Murthy. 2000. Myo-inositol metabolism in plants. *Plant Sci*., 150: 1-19.

Loewus, F.A. and M. Loewus. 1983. Myo-inositol: its biosynthesis and metabolism. Ann. Rev. *Plant Physiologyl*., 34: 137-161.

Ma, G., M, Zhang, J. Xu, W. Zhou and L. Cao. 2020. Transcriptomic analysis of short-term heat stress response in *Pinellia ternata* provided novel insights into the improved thermotolerance by spermidine and melatonin. *Ecotoxicol. Environ Saf.*, 1(202): 110877.

Ma, W., S. Wei, W. Peng, T. Sun, J. Huang, R. Yu, B. Zhang and W. Li. 2021. Antioxidant effect of *Polygonatum sibiricum* Polysaccharides in D-Galactose-Induced Heart Aging Mice. *Biomed. Res. Int*., (1): 1-8.

Meyer, M.R., F. Peters and H. Maurer. 2010. Automated mass spectral deconvolution and identification system for GC-MS screening for drugs, poisons, and metabolites in urine. *Clinical Chem.*, 56: 575-584.

Nunes, A.C., G. Vianna, F. Cuneo, J. Amaya-Farfan, G. de Capdeville, E. Rech and F. Aragao. 2006. RNAi-mediated silencing of the myo-inositol-1-phosphate synthase gene (GmMIPS1) in transgenic soybean inhibited seed development and reduced phytate content. *Planta*, 224, 125-132.

Omar, N., J. Frank, J. Kruger, F. Bello and R. Landberg. 2021. Effects of high intakes of fructose and galactose, with or without added fructooligosaccharides, on metabolic factors, inflammation, and gut integrity in a rat model. *Mol. Nutr. & Food Res*., 2001133.

Peng, Y.S., T. Li, S. Wen, G. He and S. Huang. 2016. Effect of different sand-storage methods on the germination of *Cyclobalanopsis glauca* seed. *J. Central South Uni. Forestry & Technol*., 36(8): 44-48.

Qi, J., J. Wei, D. Liao, Z. Ding, X. Yao, P. Sun and X. Li. 2022. Untargeted metabolomics analysis revealed the major metabolites in the seeds of four *Polygonatum* species. *Molecules*, 27(4): 1445.

Rubab, S., G. Rizwani, S. Bahadur, M. Shah, H. Alsamadany, Y. Alzahrani, M. Shuaib, A. Hershan, Y. Hobani and A. Shah. 2020. Determination of the GC–MS analysis of seed oil and assessment of pharmacokinetics of leaf extract of *Camellia sinensis* L. *J. King Saud Uni. Sci*., 32, 3138-3144.

Vinaixa, M., E. Schymanski, S. Neumann, M. Navarro, R. Salek and O. Yanes. 2016. Mass spectral databases for LC/MS- and GC/MS-based metabolomics: State of the field and future prospects. *Trends Anal. Chem*., 78: 23-35.

Wang, Y., X. Liu, H. Su, S. Yin, C. Han, D. Hao and X. Dong. 2019. The regulatory mechanism of chilling-induced dormancy transition from endo-dormancy to non-dormancy in *Polygonatum kingianum* Coll.et Hemsl rhizome bud. *Plant Mol Biol*., 99(3): 205-217.

Wang, Z.H., H. Jiang, J. Wang, Y. Qin and Y. Wu. 2012. Effect of sand storage on storage substance content and germination of *Polygonatum Sibiricum* Red. *Seeds*, 31(2): 91-93.

Xia, J., I. Sinelnikov, B. Han and D. Wishart. 2015. Wishart. MetaboAnalyst 3.0-making metabolomics more meaningful. *Nucl. Acids Res*., 43: W251-W257.

Xie, Y., Z. Jiang, R. Yang, Y. Ye, L. Pei, S. Xiong, S. Wang, L. Wang and S. Liu. 2021. Polysaccharide-rich extract from *Polygonatum sibiricum* protects hematopoiesis in bone marrow suppressed by triple negative breast cancer. *Biomed. Pharmacother*., 137(6): 111338.

Yang, P., X. Li, X. Wang, H. Chen, F. Chen and S. Shen. 2007. Proteomic analysis of rice (*Oryza sativa*) seeds during germination. *Proteomics*, 7: 3358-3368.

Zhang, P.F., H. Zhang, X. Zhang, Y. Yin, S. Liu, L. Li and D. Peng. 2020. Ecology suitability study of *Polygonatum cyrtonema*. *China J. Chinese Mat. Med.*, 45(13): 3073-3078.

Zhang, W., L. Xia, F. Peng, C. Song, M. Manzoor, Y. Cai and Q. Jin. 2022. Transcriptomics and metabolomics changes triggered by exogenous 6-benzylaminopurine in relieving epicotyl dormancy of *Polygonatum cyrtonema* Hua seeds. *Front Plant Sci*., 25(13): 961899.

Zhang, Y. J., Y. Zhang, F. Li, F. Liu and H. Guo. 2010. Seed Dormant characteristics of *Polygonatum sibiricum* Red. 2010. *Bull. Bot. Res.*, 30(6): 753-757.

(Received for publication 1 May 2022)